At the crossroads of astrophysics and cosmology: Period–luminosity relations in the 2020s
Proceedings IAU Symposium No. 376, 2024
R. de Grijs, P. A. Whitelock & M. Catelan, eds.
doi:10.1017/S1743921323002557

Period–Luminosity Relations in the Local Group of Galaxies

Igor Soszyński

Astronomical Observatory, University of Warsaw, Al. Ujazdowskie 4, 00-478 Warszawa, Poland. email: soszynsk@astrouw.edu.pl

Abstract. Local Group galaxies, particularly the Large and Small Magellanic Clouds, have historically played and continue to play a unique role in studies of the period–luminosity (PL), period–luminosity–color (PLC), and period–Wesenheit (PW) relations, not just for pulsating stars. In recent years, significant efforts have been devoted to calibrate the PL, PLC, and PW relationships at different wavelengths, including studies of the influence of metallicity and non-linearities on the accuracy of measured distances. However, the PL diagram has many more astrophysical applications. It serves as a vital tool for classifying different types of pulsating stars and can even facilitate the discovery of new classes of variable stars. Moreover, it aids in distinguishing among various modes of pulsation, facilitates the identification of pulsating stars that are members of binary systems, and enables studies of the three-dimensional structures of neighboring galaxies. In this contribution, I present the latest results on the PL, PLC, and PW relations obeyed by various types of variable stars in Local Group galaxies – from δ Scuti stars to Mira variabless and from close binary systems to the mysterious long secondary periods exhibited by red giant and supergiant stars.

Keywords. Cepheids, RR Lyrae stars, delta Scuti stars, Miras, binaries, stars: distances, galaxies: structure, Local Group, Magellanic Clouds

1. Introduction

Period–luminosity (PL), period–luminosity–color (PLC), and period–Wesenheit index (PW) relationships for variable stars have found many astrophysical applications, of which the most well-known is measuring distances within and beyond our Galaxy. PL, PLC, and PW relations are exhibited by pulsating stars in the Cepheid instability strip (classical Cepheids, Type II Cepheids, anomalous Cepheids, RR Lyrae stars, and δ Scuti stars), long-period variables (including Miras and semiregular variables), close binary systems, and the mysterious long secondary period variables.

The first ever PL relation was discovered in 1908 by Henrietta Swan Leavitt who studied Cepheid variables in the Small Magellanic Cloud (SMC). The Magellanic Clouds are galaxies that are located close enough so that individual stars can be easily resolved by ground-based telescopes, but far enough away that stellar populations can be treated, to first approximation, as being located at the same distance. This allows us to obtain the apparent PL relation without measuring the distances to individual Cepheids, or even without knowing the distance to their host galaxy. To date, the Magellanic Clouds, and more broadly the Local Group of galaxies, remain among the most important sources of knowledge providers about the properties of variable stars, particularly about their PL, PLC, and PW relations.

The Large Magellanic Cloud (LMC) is the nearest galaxy containing a significant stellar population, which makes it indispensable for cross-calibrating various distance indicators.

This galaxy has a very favorable position relative to us. It is located nearly face-on, which translates into a compact distribution (±1.5 kpc) of distances across the face of the galaxy (e.g., Jacyszyn-Dobrzeniecka et al. 2016). The distance to the LMC (49.59 ± 0.54 kpc) is already known with an accuracy of about 1 percent, thanks to measurements made by the Araucaria project (Pietrzyński et al. 2019) using late-type detached eclipsing binary systems. Furthermore, interstellar reddening toward the Magellanic Clouds is very accurately known thanks to the reddening maps obtained by Skowron et al. (2021) based on red clump stars.

On the contrary, the SMC exhibits a significant elongation along the line of sight, resulting in a substantial dispersion of the PL relations in this galaxy. The distance to the SMC has been determined with an accuracy of better than 2 percent based on detached eclipsing binaries (Graczyk et al. 2020). However, the SMC is characterized by significantly lower metallicity than the LMC, which, among other things, allows us to study of the influence of chemical composition on the slope and intercept of the PL relations. Considering other large galaxies of the Local Group – M31 and M33 – extends the range of investigated metallicities to values higher than those commonly found in the Milky Way.

In this contribution, various aspects of the PL, PLC, and PW relations obeyed by different types of variable stars in the galaxies of the Local Group will be presented. This work focuses not only on classical Cepheids and not only on distance measurements but also demonstrates a wide range of applications of the PL relationships in astrophysics. Examples of the latest studies of neighboring galaxies that allow us to learn about the properties of variable stars will be presented, as well as examples of how the PL relationships allow us to learn about the structure of nearby galaxies. This article is divided into sections describing various types of variable stars that follow PL relations. All figures showing the PL and PW diagrams and example light curves of variable stars have been generated using photometric data gathered by the Optical Gravitational Lensing Experiment (OGLE) survey (Udalski et al. 2015a).

2. Classical Cepheids

The PL relation for classical Cepheids was, for the first time, mentioned by Leavitt (1908) in her paper describing the catalog of variable stars in the Magellanic Clouds. "It is worthy of notice that in Table IV the brighter variables have the longer periods" – this sentence describing the properties of 16 variables in the SMC is considered an announcement of the discovery of the PL relation for Cepheids, today known as the 'Leavitt Law'. The PL relation was first plotted on a graph in the paper by Leavitt & Pickering (1912). Since then, efforts have been made to calibrate the Leavitt Law to absolute magnitudes (e.g., Hertzsprung 1913; Shapley 1918) in order to use Cepheids as standard candles for measuring distances. A decade later, this led to the measurement of the distances to M31 and M33 (Hubble 1925), ultimately confirming the hypothesis of the Island Universe, and then to the discovery of the expansion of the Universe (Hubble 1929).

Over the next decades, the Leavitt Law was calibrated increasingly accurately, with the most significant revision of the distance scale made by Baade (1956). Until the 1990s, most PL diagrams for classical Cepheids showed only one relationship, populated by the fundamental-mode pulsators (e.g., Sandage & Tammann 1968; Madore 1982). The physical nature of so-called sinusoidal or s-Cepheids was subject of debate for years (e.g., Arp 1960; Ivanov & Nikolov 1976; Connolly 1980). A breakthrough came in the 1990s with the launch of large-scale sky surveys aimed primarily at searching for gravitational microlensing events, but their side products were huge photometric databases ideally suited for large-scale studies of variable stars. After several years of observations, the EROS (Beaulieu et al. 1995), MACHO (Alcock et al. 1995) and OGLE (Udalski et al.

https://doi.org/10.1017/S1743921323002557 Published online by Cambridge University Press

1999) projects presented PL and PW diagrams for classical Cepheids in the Magellanic Clouds. Two parallel relationships were clearly visible, finally confirming that s-Cepheids are first-overtone pulsators.

The top panel of Figure 1 displays the modern PW diagram for classical Cepheids in the LMC. Four relationships can be distinguished, for stars pulsating in the fundamental and the first three overtone modes (the third overtone occurs only in multi-mode pulsators). This diagram was obtained based on long-term observations in the I and V bands carried out by the OGLE project – the only still active sky survey of those pioneering microlensing projects which started over 30 years ago. Throughout its long history, OGLE has evolved and currently, in the fourth phase of the project (OGLE-IV), regularly observes about two billion stars in the densest regions of the southern sky: the Galactic bulge and disk, the LMC and SMC, in total about 3600 square degrees across the sky. Since 1997, the survey has been conducted with the dedicated 1.3 m Warsaw Telescope located at Las Campanas Observatory in Chile.

Variable stars occupy a special position among the most important achievements of the OGLE project. The OGLE Collection of Variable Stars (OCVS) currently contains more than a million variable objects, mainly pulsating stars and eclipsing binaries. Among others, this catalog contains over 10,000 Cepheids of various types in the Magellanic Clouds (Soszyński et al. 2018, 2019b), which is a virtually complete list of such objects in these galaxies. The OCVS is characterized by a very high level of completeness and purity, since the final decision on the classification of each variable star is made by an experienced astronomer after visual inspection of the light curves. Therefore, the OCVS serves as a framework for various astrophysical studies, including many papers presented in these proceedings.

2.1. *Classical Cepheids as Standard Candles*

This presentation of the latest results pertaining to classical Cepheids will begin with their canonical role as distance indicators. Since the LMC is an anchor galaxy for the cosmic distance scale, the Leavitt Law in this galaxy has been studied over a wide range of wavelengths, from the optical to the mid-infrared domain (e.g., Ngeow et al. 2009; Macri et al. 2015; Chown et al. 2021).

One of the most remarkable calibrations of the Leavitt Law in recent years was presented by Riess et al. (2019). They used observations from the *Hubble Space Telescope* (*HST*) to study the PL and PW relations followed by 70 long-period Cepheids in the LMC. This was a significant achievement, because the same photometric system had been used earlier to measure distances to galaxies hosting Type Ia supernovae, resulting in a more precise determination of the Hubble constant, H_0. Calibrating LMC Cepheids with *HST* observations was a major research challenge due to the *HST* camera's small field of view ($2'$), implying that only a single Cepheid could typically be observed per image. The authors overcame this limitation by designing a new observation mode that used the *HST* gyroscopes for both slewing and guiding. Additionally, the *HST* has faced significant technical problems related to its gyroscopes, which made the observations even more challenging.

The Riess et al. (2019) calibration of the Leavitt Law in the *HST* passbands has already been employed to measure the distances to the Local Group galaxies M31 (Li et al. 2021) and M33 (Breuval et al. 2023) with unprecedented accuracy of 1.5% and 1.3%, respectively. Both galaxies are among the best sites for cross-calibrating various distance indicators, making them strong candidates as new anchors for the cosmic distance scale.

Achieving accurate calibrations of the PL relations for Cepheids, which is essential for measuring the Hubble constant with an accuracy of better than 1%, requires a

https://doi.org/10.1017/S1743921323002557 Published online by Cambridge University Press

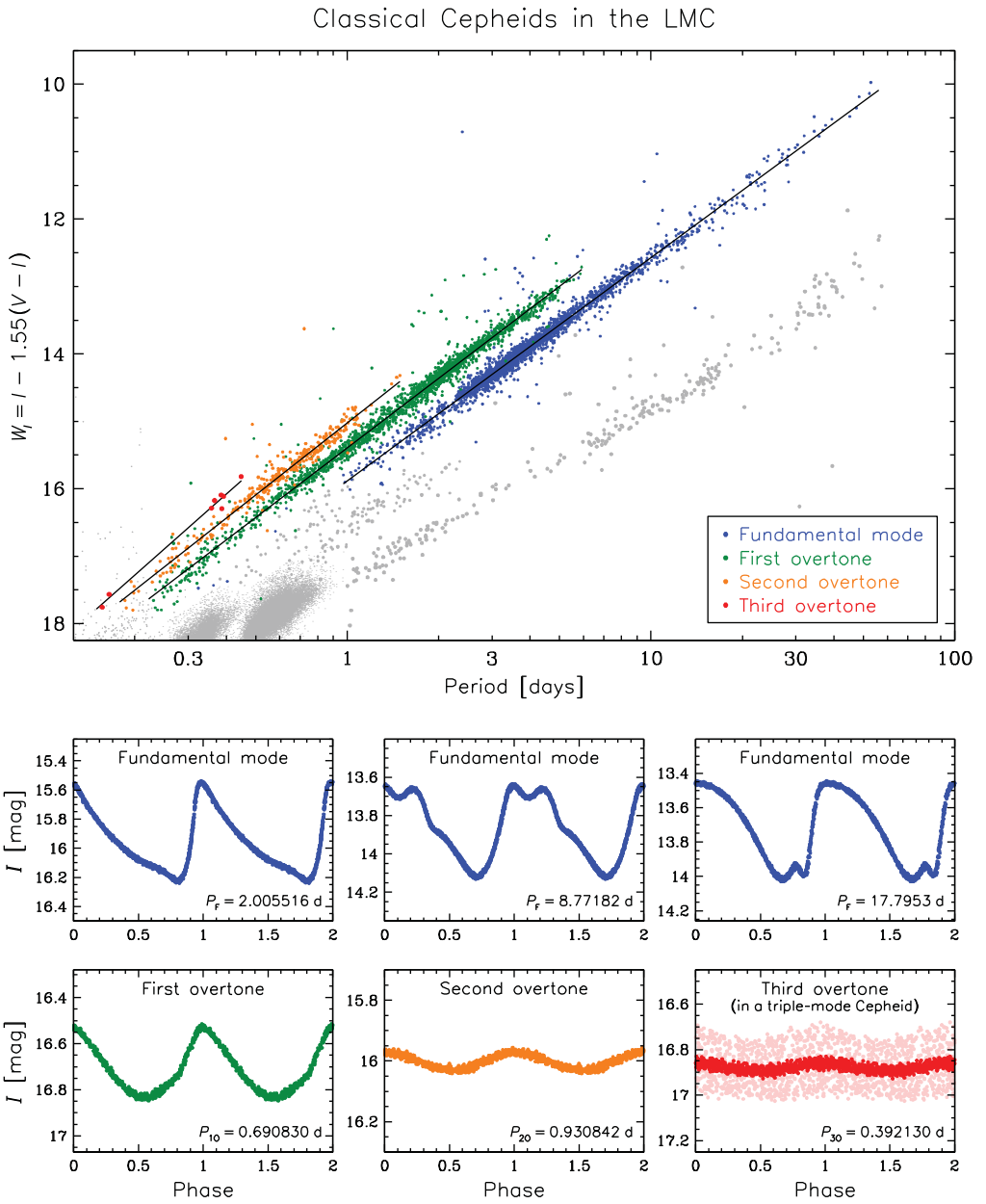

Figure 1. (top) Period–Wesenheit index diagram for classical Cepheids in the LMC (Soszyński et al. 2017, 2019b). The Wesenheit index is an extinction-free quantity defined as $W_I = I - 1.55(V - I)$, where the I- and V-band mean magnitudes of the Cepheids originate from the OGLE-IV survey (Udalski et al. 2015a). Blue, green, orange, and red dots mark the fundamental, first-, second-, and third-overtone pulsation modes, respectively, in both single-mode and multimode Cepheids. Gray points indicate other types of classical pulsators: Type II Cepheids, anomalous Cepheids, RR Lyrae stars, and δ Scuti stars. (bottom) Typical I-band light curves of classical Cepheids pulsating in different modes. The third overtone is only observed in double- and triple-mode Cepheids.

https://doi.org/10.1017/S1743921323002557 Published online by Cambridge University Press

comprehensive understanding of potential systematic errors. These errors may arise from factors such as non-linearities in the PL relations or their dependence on metallicity.

The non-linearity of the Cepheid PL relation has been the subject of numerous studies over the past years (e.g., Kanbur et al. 2007; Ngeow et al. 2008; García-Varela et al. 2013). For instance, Bhardwaj et al. (2016) performed a statistical analysis of potential non-linearities in the PL, PW, and period–color relations obeyed by LMC classical Cepheids in optical and infrared bands. They applied various statistical tests to evaluate the significance of the non-linearities and found a small but statistically significant change in the slope of the PL and PW relations at $P = 10$ d for fundamental-mode Cepheids and at $P = 2.5$ d for first-overtone pulsators. The near-infrared period–W_{HK} relation, however, was found to be perfectly linear for both fundamental-mode and first-overtone Cepheids. Generally, the impact of possible non-linearities in the PL relations on extragalactic distance determinations and H_0 measurements was estimated to be marginal.

In addition, the chemical abundance of Cepheids has a significant contribution to the error budget of the Hubble constant. Therefore, in recent years, a lot of effort has been put into solving this problem (e.g., Wielgórski et al. 2017; Gieren et al. 2018; Groenewegen 2018; Ripepi et al. 2020; Breuval et al. 2021). The metallicity–luminosity relation for Cepheids is taken into account by including a corrective term, γ, in the PL relation:

$$M_\lambda = \alpha \log P + \beta + \gamma[\mathrm{Fe/H}]. \quad (1)$$

Various estimates of the γ values have been published in recent years. At present, most authors agree that this coefficient is negative, which means that metal-rich Cepheids are brighter than metal-poor ones. However, the dispersion in the measured values of the γ term is still significant, indicating that even after decades of research the metallicity effect on the Cepheid PL relation is not well-understood.

In their recent work, Breuval et al. (2022) compared the absolute PL relations for classical Cepheids in the Milky Way, LMC, and SMC, with the aim of deriving the metallicity effect in 10 filters covering the wavelength range of 0.5–4.5 μm. The authors took advantage of the fact that the iron abundance, [Fe/H], of young stellar populations in these three Local Group galaxies differs significantly, ranging from -0.75 to $+0.088$ dex. As a result, a uniform value of the γ term of about -0.28 mag dex^{-1} from optical to mid-infrared wavelengths was obtained.

2.2. *Cepheids in Binary Systems*

The PL relations for Cepheids in the Local Group are used for more than just calibrating the extragalactic distance scale. An original application of the PL diagram was proposed by Pilecki et al. (2021), who selected 41 classical Cepheids in the LMC lying at least 0.44 mag above the PL relation corresponding to their pulsation mode. In other words, they analyzed Cepheids that were at least 50% brighter than other Cepheids at the same pulsation period. The project aimed to extend the list of known classical Cepheids that are members of double-lined binaries beyond the eclipsing systems containing Cepheids discovered by the OGLE project (Pietrzyński et al. 2010; Udalski et al. 2015b).

Preliminary spectroscopic observations of 18 Cepheids from this overluminous sample revealed 16 double-lined binaries (Pilecki et al. 2021). Further observations led to the discovery of a Cepheid in a binary system with an orbital period of only 59 days, five times shorter than any such period measured before (Pilecki et al. 2022). Currently, 56 candidate Cepheids in the LMC, SMC, and Milky Way have been confirmed to reside in double-lined systems (B. Pilecki, private communication; see also these proceedings). The

https://doi.org/10.1017/S1743921323002557 Published online by Cambridge University Press

orbital motions of the Cepheids and their companions were detected in 32 of these systems. Moreover, eight of the confirmed systems are composed of two Cepheids. Such binary systems are excellent laboratories for testing evolutionary models of classical pulsators.

2.3. *Three-Dimensional Structure of Galaxies*

Studies of the three-dimensional geometry of Local Group galaxies, such as the LMC and SMC, are crucial to understand past interactions between star systems in the immediate vicinity of the Milky Way. Many investigations of the Magellanic System's spatial structure have been performed based on the PL relations of classical Cepheids (e.g., Inno et al. 2016; Jacyszyn-Dobrzeniecka et al. 2016; Ripepi et al. 2017; Deb et al. 2018). Here, I present the newest research by Ripepi et al. (2022), who used the OGLE Collection of Cepheids in the LMC (Soszyński et al. 2017) with time-series near-infrared photometry obtained by the VISTA Survey of the Magellanic Clouds (VMC; Cioni et al. 2011) to study the three-dimensional geometry of the young population in the LMC.

The near-infrared PL and PW relations obtained by Ripepi et al. (2022) are spectacularly narrow thanks to the deep VMC photometry and relatively good sampling of the light curves (typically 15–30 epochs). Thanks to the small dispersions in the PL relations, the distances to individual Cepheids were determined with a precision of about 1 kpc (2%). As a result, the authors presented accurate three-dimensional maps of the LMC, analyzed various substructures within this galaxy, measured the scale height of the disk, and derived the viewing angles of the LMC bar and disk. Additionally, Ripepi et al. (2022) reported the discovery of a new non-linearity in the PL relationship for first-overtone Cepheids with a break at $P = 0.58 \pm 0.1$ d, but the same nonlinearity (at $P = 0.5$ d) was earlier noticed by Soszyński et al. (2008a).

3. Type II Cepheids

Until the mid-20th century, astronomers were unaware of the existence of more than one type of Cepheid variable. The major revision of the distance scale made by Baade (1952) directly led the division of Cepheids into classical and Type II objects. The latter group is composed of low-mass stars belonging to the halo and old disk populations. Traditionally, Type II Cepheids are classified into BL Herculis (with pulsation periods in the range of 1–4 d), W Virginis (4–20 d), and RV Tauri stars (> 20 d). Additionally, Soszyński et al. (2008b) proposed a new subtype, dubbed peculiar W Virginis stars, which have light curves of different shapes and are bluer and brighter than ordinary W Virginis stars. A large fraction of peculiar W Virginis variables show signs of binarity, such as eclipsing or ellipsoidal modulation of their light curves. Therefore, it is probable that the pulsation of these stars is a consequence of their evolution in close binary systems.

3.1. *PL Relation for Type II Cepheids*

Type II Cepheids exhibit well-defined PL and PW relationships (Figure 2). These stars are 1.5–2 mag fainter than classical Cepheids at similar periods, but they are 1–4 mag brighter than RR Lyrae stars, which makes them useful distance indicators in environments where classical Cepheids are not present, such as globular clusters or dwarf spheroidal galaxies.

The most recent calibration of the PL relation for Type II Cepheids in the Milky Way and the LMC was published by Wielgórski et al. (2022). In the Milky Way, they used about 20 nearby BL Herculis and W Virginis stars along with their parallaxes from *Gaia* Data Release (DR) 3, while in the LMC, the sample of Type II Cepheids was

https://doi.org/10.1017/S1743921323002557 Published online by Cambridge University Press

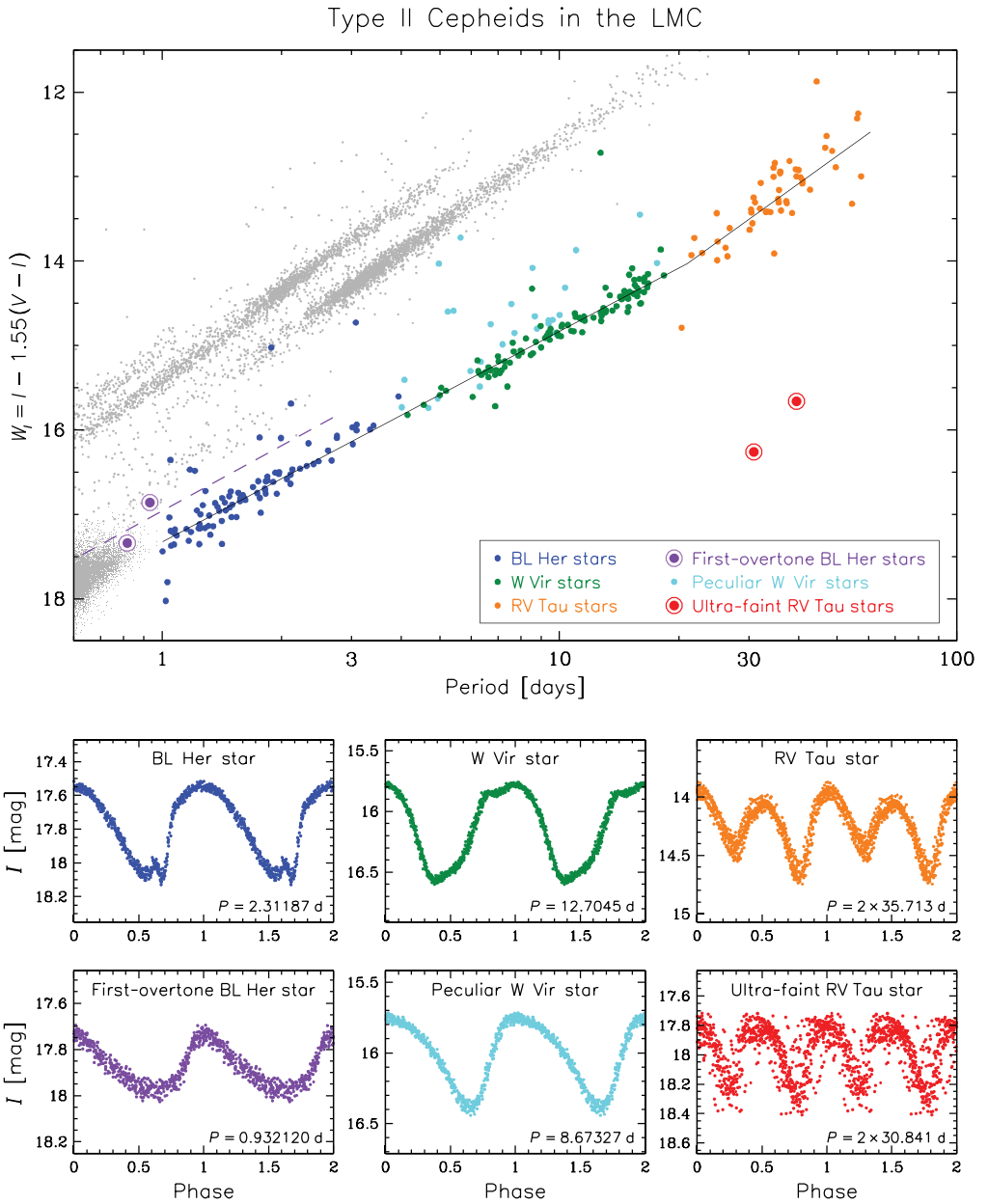

Figure 2. (top) PW diagram for Type II Cepheids in the LMC (Soszyński et al. 2018). Different types of classical pulsators are color coded: blue for fundamental-mode BL Herculis stars, green for W Virginis stars, orange for RV Tauri stars, purple for first-overtone BL Herculis stars (Soszyński et al. 2019a), cyan for peculiar W Virginis stars (Soszyński et al. 2008b), red for ultra-faint RV Tauri stars (Soszyński et al. 2018), and gray for other types of classical pulsators. (bottom) Example I-band light curves of different classes of Type II Cepheids.

taken from the OCVS (Soszyński et al. 2018). The slopes of the near-infrared relations in the Milky Way and LMC were found to be slightly different, at the level of 2σ. Additionally, Wielgórski et al. (2022) noticed a significant metallicity effect of about -0.2 mag dex^{-1}, indicating that metal-rich Type II Cepheids are intrinsically brighter

https://doi.org/10.1017/S1743921323002557 Published online by Cambridge University Press

than their metal-poor counterparts. Interestingly, the sign of this relation is opposite to that of RR Lyrae stars (e.g., Neeley et al. 2019), which may indicate that the common PL relation obeyed by RR Lyrae variables and Type II Cepheids in the LMC (Bhardwaj et al. 2017) is not a universal feature.

3.2. *First-Overtone Type II Cepheids*

For years, all Type II Cepheids were believed to be exclusively fundamental-mode pulsators, until Smolec et al. (2018) identified the first two cases of BL Herculis stars pulsating simultaneously in the fundamental and first-overtone modes. To date, a total of five double-mode Type II Cepheids have been identified in the Milky Way (Udalski et al. 2018; Soszyński et al. 2020). These stars form a very homogeneous class of pulsators, with their fundamental-mode periods ranging from 1.0 to 1.4 d and their period ratios ranging between 0.70 and 0.71.

Inspired by the discovery of multimode Type II Cepheids, Soszyński et al. (2019a) conducted a search for BL Herculis stars pulsating solely in the first overtone. The primary tool used for this task was the PL diagram for classical pulsating stars in the LMC. First-overtone Type II Cepheids should be located in close proximity to the purple dashed line in Figure 2, corresponding to a period ratio of 0.7 between the first overtone and the fundamental mode. Additionally, potential candidates for first-overtone BL Herculis stars should have light curves exhibiting features typical of overtone pulsators, in particular round minima. A search of the OGLE photometric database of the LMC revealed two stars fitting these criteria: OGLE-LMC-T2CEP-290 and OGLE-LMC-T2CEP-291. Their positions in the PW diagram are marked with purple circles in the top panel of Figure 2, while the bottom left panel of this figure shows the light curve of one of these stars (OGLE-LMC-T2CEP-290). Three other candidates for first-overtone Type II Cepheids were subsequently discovered in the Milky Way (Soszyński et al. 2020).

3.3. *Ultra-Faint RV Tauri Stars*

Another example of unique objects discovered in the PL diagram are two ultra-faint RV Tauri stars in the LMC (Soszyński et al. 2018). The light curves of OGLE-LMC-T2CEP-207 and OGLE-LMC-T2CEP-237 exhibit typical features of RV Tauri stars, including slight variations in pulsation period, long-period modulation of the mean brightness in the case of OGLE-LMC-T2CEP-207 (a characteristic of RVb stars), and small but detectable alternations of deeper and shallower minima. These stars also have a $(V-I)$ color index consistent with RV Tauri variables. However, they are roughly 2.5 mag fainter than other RV Tauri stars in the LMC (red circles in the top panel of Figure 2). A possible explanation of the nature of these ultra-faint RV Tauri stars is that they are post-red-giant-branch stars (Manick et al. 2018), as opposed to classical RV Tauri stars that are thought to be post-asymptotic-giant-branch stars.

4. Anomalous Cepheids

The term 'anomalous' Cepheids was coined by Zinn & Searle (1976) to describe a class of pulsating stars whose properties did not match those of classical or Type II Cepheids. Anomalous Cepheids are radially pulsating stars that burn helium in their cores and have low metal content, with masses between 1 and 2 $M_{\odot}$ (Bono et al. 1997; Marconi et al. 2004; Groenewegen & Jurkovic 2017). In the PL plane, they occupy the region between the relations of classical and Type II Cepheids (Figure 3).

Just 15 years ago, only a few dozen anomalous Cepheids were known, the vast majority found in nearby dwarf galaxies. Very few such stars were known in Galactic globular

https://doi.org/10.1017/S1743921323002557 Published online by Cambridge University Press

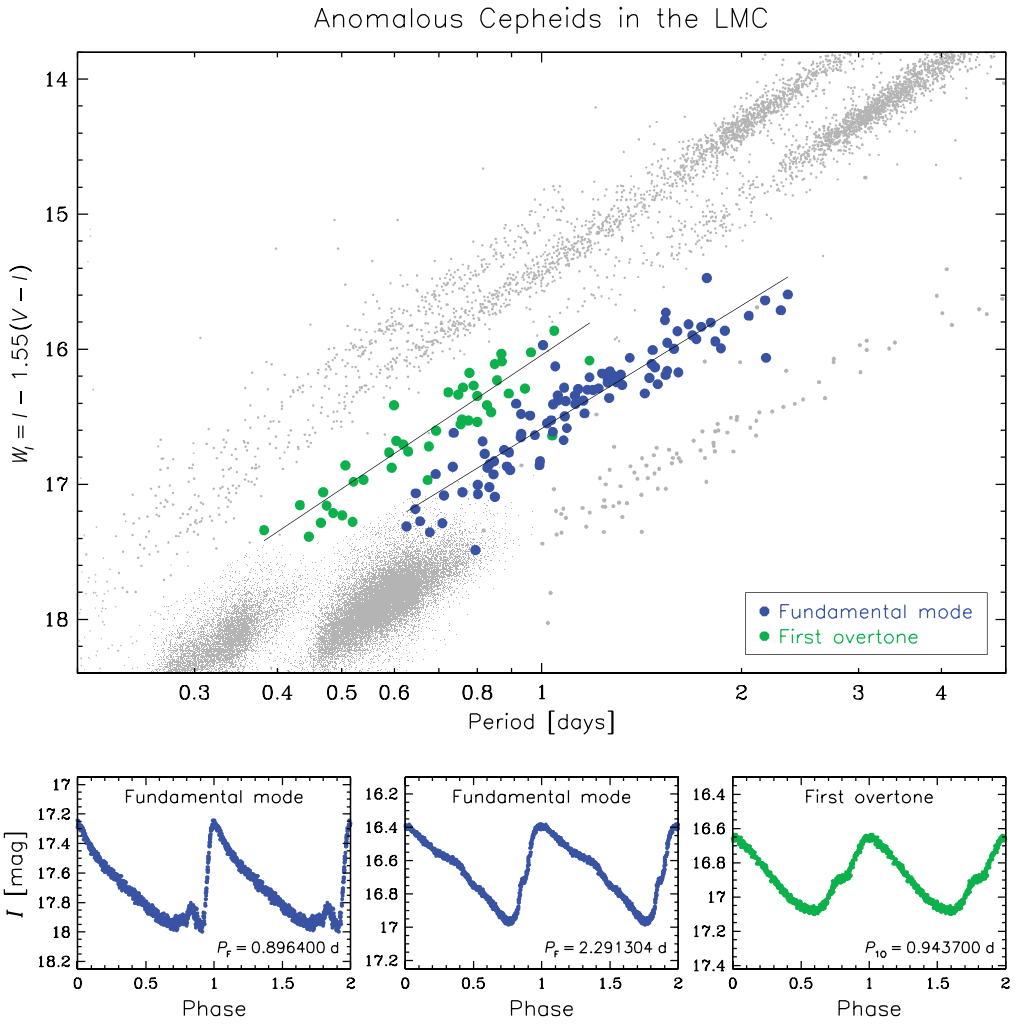

Figure 3. (top) Period–Wesenheit index diagram for anomalous Cepheids in the LMC (Soszyński et al. 2015, 2019b). Blue circles indicate fundamental-mode pulsators, while green symbols mark first-overtone Cepheids. Gray dots show the positions of classical Cepheids, Type II Cepheids, and RR Lyrae stars. (bottom) I-band light curves of typical anomalous Cepheids in the LMC.

clusters and only one anomalous Cepheid, XZ Ceti, was known in the field of the Milky Way (Szabados et al. 2007). However, this situation changed when the OGLE team first reported the discovery of 80 (Soszyński et al. 2008b) and later more than 260 anomalous Cepheids in the LMC and SMC (Soszyński et al. 2015, 2019b). The position of these stars in the PL diagram was the primary criterion that allowed us to separate anomalous Cepheids from classical Cepheids, Type II Cepheids, and RR Lyrae stars.

With this large and homogeneous sample of anomalous Cepheids in the Magellanic Clouds, Soszyński et al. (2015) developed a method for distinguishing them from other types of classical pulsating stars based on the light curve morphology, using the ϕ_{21} and ϕ_{31} parameters of the Fourier light curve decomposition. The period–Fourier coefficient diagram proved to be effective tools for identifying different types of Cepheids, both fundamental-mode and first-overtone ones. By applying this method,

https://doi.org/10.1017/S1743921323002557 Published online by Cambridge University Press

Soszyński et al. (2015, 2020) detected approximately 120 anomalous Cepheids in the Milky Way. This way, the PL diagram for pulsating stars in the Magellanic Clouds enabled the identification of a significant number of anomalous Cepheids in our own Galaxy.

Ripepi et al. (2019) presented a similar application for the PL diagram for pulsating stars in the Magellanic Clouds, using different types of variables in these galaxies to improve the classification of Milky Way Cepheids included in the *Gaia* DR2 catalog of variable stars.

5. RR Lyrae Stars

RR Lyrae variables are the most abundant type of classical pulsators, with hundreds of thousands of stars of this type known across the Universe. Tens of thousands of them have been found in the galaxies of the Local Group (e.g., Soszyński et al. 2019b; Clementini et al. 2022; Nagarajan et al. 2022), including nearly 50,000 identified in the Magellanic System (Figure 4). RR Lyrae stars are old (> 10 Gyr) and low-mass (< 0.85 $M_\odot$) stars that occupy the intersection of the instability strip with the horizontal branch. They are a perfect tool to trace the oldest stellar component and probe the structure of galactic halos. When using RR Lyrae stars as distance indicators, it is essential to consider the dependence of their brightness on metallicity. In other words, period–luminosity–metallicity (PLZ) relations should be used (e.g., Borissova et al. 2009; Muraveva et al. 2015; Bhardwaj et al. 2023).

The usefulness of the PLZ relations for RR Lyrae stars extends beyond measuring distances to star clusters and nearby galaxies. When distances are known from independent measurements, the PLZ relationship can be inverted to calculate the metallicities of individual RR Lyrae stars and trace the early chemical evolution of their host systems (e.g., Braga et al. 2016; Martínez-Vázquez et al. 2016). Moreover, when photometric observations in several optical and near-infrared bands are available, it is possible to simultaneously measure the distance, metallicity, and reddening of RR Lyrae stars (Bono et al. 2019). The versatile properties of RR Lyrae stars are commonly used to study the spatial structure, star formation history, and metallicity gradients in neighboring galaxies (e.g., Deb & Singh 2014; Jacyszyn-Dobrzeniecka et al. 2017; Muraveva et al. 2018; Ferguson & Strigari 2020).

In one of the most recent analyses, Cusano et al. (2021) studied the three-dimensional geometry of the LMC as traced by 29,000 RR Lyrae stars from the OGLE (Soszyński et al. 2016a, 2019b) and *Gaia* DR2 (Clementini et al. 2019) catalogs supplemented with near-infrared observations from the VMC survey. The LMC structure visible in old stars has a triaxial ellipsoid shape with axis ratios of 1:1.2:1.8 and no additional substructures.

6. δ Scuti Stars

δ Scuti variables are the faintest members of the family of classical pulsators. They are intermediate-mass stars (1.5–2.5 $M_\odot$) that pulsate in low-order radial or non-radial modes with periods of up to 0.3 d. In the Hertzsprung–Russell diagram, they lie close to the intersection of the Cepheid instability strip with the main sequence. δ Scuti pulsators consist of a mixture of stars in different evolutionary stages, including pre-main-sequence, main-sequence, and post-main-sequence stars, as well as blue stragglers (which are known as SX Phoenicis stars).

Due to the low intrinsic brightness of δ Scuti stars, most empirical efforts to measure their PL relations have relied on nearby objects with well-determined parallaxes (e.g.,

https://doi.org/10.1017/S1743921323002557 Published online by Cambridge University Press

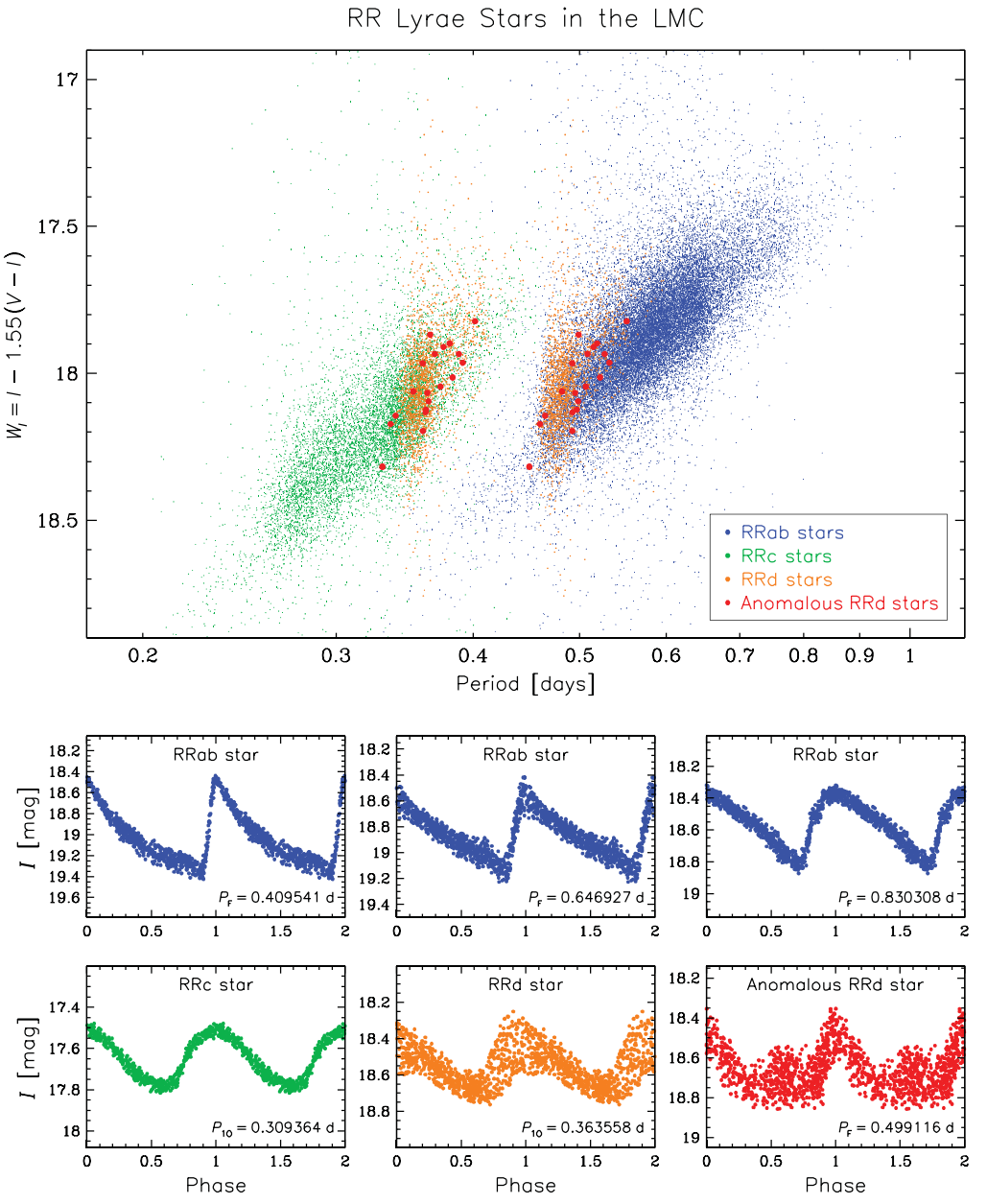

Figure 4. (top) Period–Wesenheit index diagram for RR Lyrae stars in the LMC (Soszyński et al. 2016a, 2019b). RRab stars are marked with blue points, RRc stars with green points, RRd stars with yellow points, and anomalous RRd stars (Soszyński et al. 2016b) with red circles. Each double-mode (RRd) star is represented by two points corresponding to the two pulsation periods. (bottom) Example I-band light curves of different types of RR Lyrae variables.

Ziaali et al. 2019; Jayasinghe et al. 2020; Barac et al. 2022) or on SX Phoenicis variables in Galactic globular clusters, whose distances have been independently determined using other distance indicators (e.g., Cohen & Sarajedini 2012; Ngeow et al. 2023). Until recently, the largest existing catalogs of extragalactic δ Scuti stars contained in total

https://doi.org/10.1017/S1743921323002557 Published online by Cambridge University Press

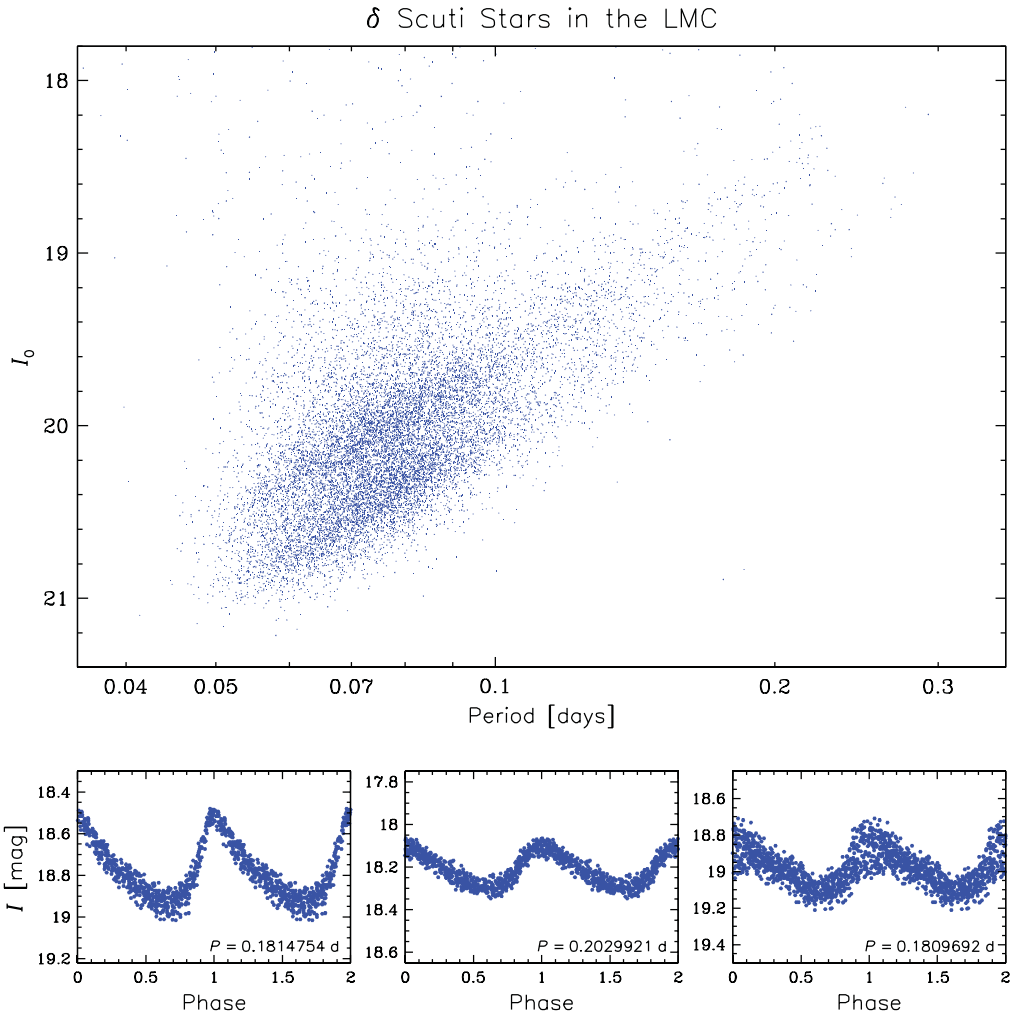

Figure 5. (top) I-band period–luminosity diagram for about 15,000 δ Scuti stars in the LMC (Soszyński et al. 2023). The magnitudes have been corrected for interstellar extinction using the reddening maps of Skowron et al. (2021). (bottom) Example I-band light curves of δ Scuti variables in the LMC.

several thousand objects in the LMC (Garg et al. 2010; Poleski et al. 2010) and SMC (Soszyński et al. 2022). This situation has been improved thanks to the recent publication of more than 15,000 δ Scuti stars in the LMC detected in the OGLE-IV database (Soszyński et al. 2023).

Before this publication, Martínez-Vázquez et al. (2022) used the available sources of extragalactic δ Scuti stars to investigate their distribution in the PL plane. The authors presented a single PL sequence that showed a significant change in slope at a pulsation period of approximately 0.09 d. However, analysis of the new OGLE-IV collection of δ Scuti pulsators in the LMC (Soszyński et al. 2023) does not confirm this conclusion. The extended sample is consistent with two linear PL relationships corresponding to the fundamental and first-overtone pulsation modes (Figure 5). It appears that the segmented PL relation reported by Martínez-Vázquez et al. (2022) was an illusion resulting from incompleteness of the available catalogs of extragalactic δ Scuti stars.

https://doi.org/10.1017/S1743921323002557 Published online by Cambridge University Press

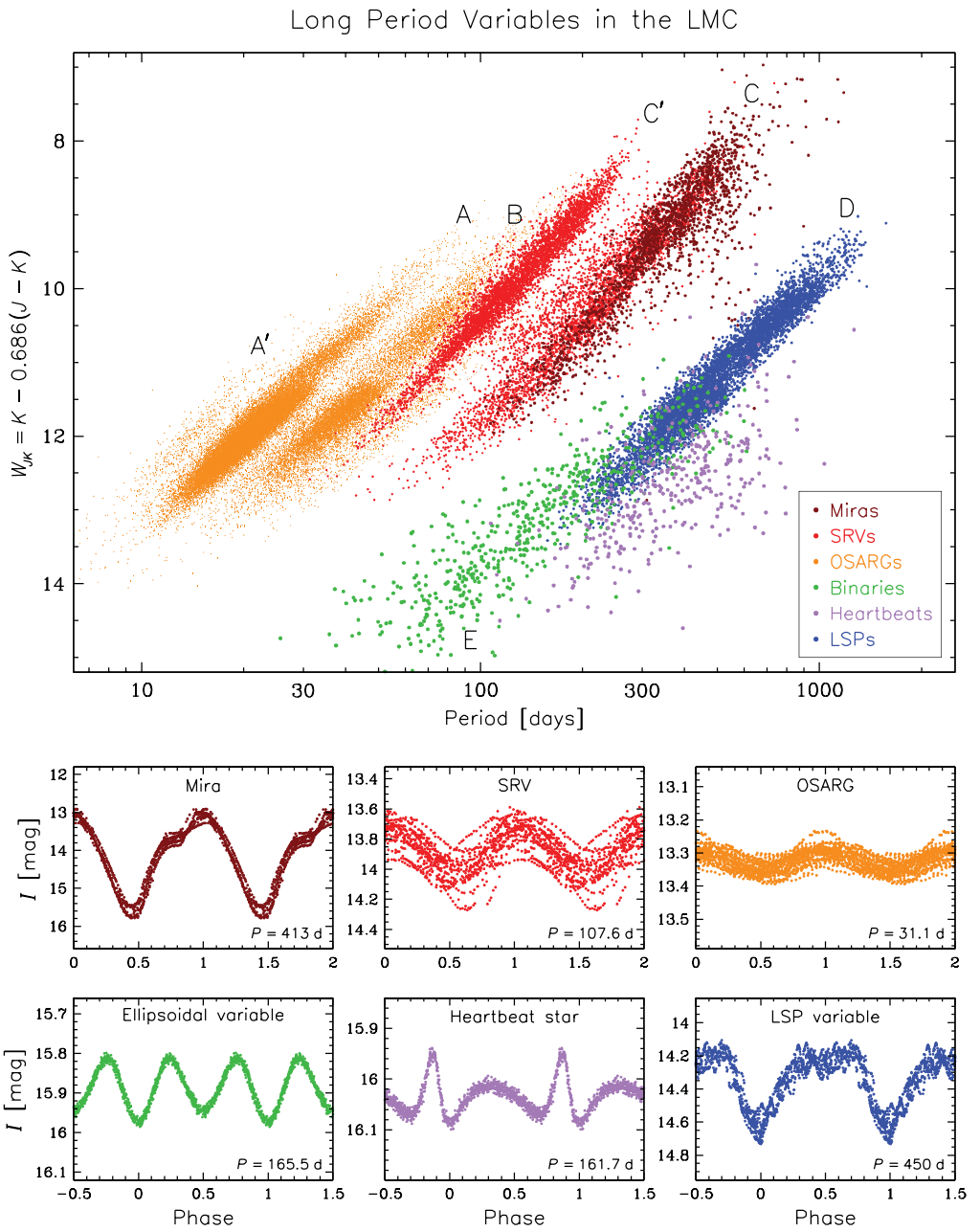

Figure 6. (top) Near-infrared period–Wesenheit index diagram for LPVs in the LMC (Soszyński et al. 2009). The near-infrared Wesenheit index is defined as $W_{JK} = K_s - 0.686\,(J - K_s)$, where the J- and K_s-band magnitudes originate from the IRSF Catalog (Kato et al. 2007) or the 2MASS Catalog (Cutri et al. 2003). Different colors of the points indicate different types of LPVs: brown – Miras, red – SRVs, orange – OSARGs, green – eclipsing and ellipsoidal close binary systems containing a red giant as one of the components, lavender – heartbeat stars, and blue – LSP variables. (bottom) Typical I-band light curves of various types of LPVs.

https://doi.org/10.1017/S1743921323002557 Published online by Cambridge University Press

7. Long-Period Variables

Long-period variables (LPVs) are pulsating stars belonging to either the red giant branch (RGB), asymptotic giant branch (AGB), or red supergiant branch. They are typically classified into three groups: Miras, semi-regular variables (SRVs), and OGLE small-amplitude red giants (OSARGs). The distribution of LPVs in the PL and PW planes is one of the primary tools for studying the physics and evolution of red giant stars.

Historically, the most important discoveries in the PL diagrams of LPVs have been made by studying variables in the LMC. Glass & Lloyd Evans (1981) were the first to demonstrate that Miras in the LMC follow a narrow PL relation in the infrared. Later, Wood & Sebo (1996) showed that SRVs follow the same PL sequence as Miras and additionally obey a second, parallel relation at shorter periods, which is today attributed to the first-overtone pulsation mode. The revolution in the PL diagram came with the advent of the microlensing sky surveys such as MACHO and OGLE, which published large samples of LPVs in the Magellanic Clouds. Wood et al. (1999) discovered five PL sequences for LPVs and labeled them with the letters A to E (with Miras lying along sequence C). Since then, the number of PL relationships for pulsating red giants has increased even more (e.g., Soszyński et al. 2007). Figure 6 depicts the contemporary near-infrared PW diagram for LPVs in the LMC, where the periods have been taken from the OCVS (Soszyński et al. 2009), while the near-infrared Wesenheit index was derived using photometric measurements from the IRSF (Kato et al. 2007) or 2MASS (Cutri et al. 2003) catalogs.

7.1. *Miras as Distance Indicators*

LPVs embody an interesting alternative to Cepheids as indicators of the extragalactic distance scale. Pulsating red giants are a numerous class of variable stars, they are bright at infrared wavelengths, and present in all types of galaxies. The vast majority of attempts to use the PL relations of LPVs to measure distances have used Mira variables (e.g., Yuan et al. 2018; Huang et al. 2020; Ou et al. 2023).

Iwanek et al. (2021) obtained the most precise PL relationships for Mira stars in mid-infrared bands using data from the *WISE* (Wright et al. 2010) and *Spitzer* (Werner et al. 2004) space telescopes. These PL sequences proved useful in determining the distances to individual oxygen- and carbon-rich Miras with an accuracy of 5% and 12%, respectively. In a subsequent study, Iwanek et al. (2023) applied these relations to the OGLE-IV collection of Mira stars (Iwanek et al. 2022) to map the central regions of the Milky Way.

The PL relations for LPVs are typically studied in infrared bands, since the light of Miras is affected by extinction from circumstellar dust that usually accompanies large-amplitude pulsations. However, Bhardwaj et al. (2019) analyzed the OGLE I- and V-band light curves of Miras in the Magellanic Clouds and found that the PLC relation in optical bands can also be quite narrow, similar to that at infrared wavelengths, particularly when the maximum brightness is used instead of the mean luminosity of individual stars.

7.2. *PL Relations for Red Supergiants*

Red supergiant stars also follow the PL relations, making them promising extragalactic distance tracers, especially since they are several magnitudes brighter than the tip of the RGB (TRGB). Ren et al. (2019) analyzed time-series photometry of red supergiants in M31 and M33 collected by the intermediate Palomar Transient Factory (iPTF) survey.

https://doi.org/10.1017/S1743921323002557 Published online by Cambridge University Press

In both galaxies, red supergiant stars formed two distinct PL relationships corresponding to the fundamental and first-overtone modes.

Interestingly, the relative number of the fundamental-mode and first-overtone red supergiants in M31 and M33 differed. Extending this study to other Local Group galaxies (the Milky Way, LMC, and SMC) revealed that this was not a coincidence. There is a strong correlation between metallicity and the relative number of red supergiants pulsating in different modes. In the metal-poorest SMC, all supergiants are first-overtone pulsators, but the fraction of fundamental-mode variables increases with increasing metallicity, reaching more than 80% in the most metal-rich M31. Ren et al. (2019) suggested that this correlation may be related to convection since high metallicity leads to less effective radiative transfer due to higher opacity, and consequently, stronger convection is required, which then affects the preferred pulsation mode.

7.3. *Potential of SRVs and OSARGs as Distance Indicators*

Trabucchi et al. (2021) tested the potential of SRVs as standard candles. They found that some SRVs exhibit the same PL relationship as Miras and can therefore be used successfully to measure distances. However, the untapped potential of the PL sequences followed by OSARG variables is worth noting. Although analysis of the pulsation periods of these stars requires a larger number of observations than for Mira variables due to their multi-period nature and smaller amplitudes, OSARGs have other advantages. They are two orders of magnitude more numerous than Miras, and their light curves are less affected by circumstellar matter due to their reduced mass loss. Identification of pulsation modes in OSARGs would be an ideal task for artificial intelligence algorithms.

An interesting application of OSARGs was recently presented by Anderson et al. (2023), who reported absolute calibration of the TRGB distance scale with an unprecedented accuracy of 1.4%. The authors used OSARG variables in the LMC, carefully selected in the PL diagram by the OGLE team (Soszyński et al. 2009). This method produced more accurate calibration of the TRGB compared to the calibration based on the general RGB population. Anderson et al. (2023) used their calibration to derive the Hubble constant and obtained better than 1σ agreement with the Cepheids-based H_0 value.

8. Close Binary Systems

Since the pioneering works of Rucinski (1994) and Rucinski & Duerbeck (1997), it has been established that contact binaries follow the PL and PLC relations due to the correlation between the size of the components and the radius of the orbit (e.g., Chen et al. 2016, 2018; Ngeow et al. 2021). Pawlak (2016) used a sample of contact and nearly-contact massive binary systems in the LMC to calibrate their PLC relationship. One of the conclusions of this study was that massive contact binaries follow a different PLC relation than low-mass W UMa stars (e.g., Rucinski 2004), indicating that the PLC relation for the entire population of contact binaries is non-linear.

In turn, Pawlak et al. (2014) investigated close binaries (eclipsing systems and ellipsoidal variables) with a red giant star as one of the components that form the PL relation known as sequence E (Wood et al. 1999). While this sequence is generally wider than other PL relations followed by LPVs (Figure 6), the dispersion in sequence E can be significantly reduced by considering ellipsoidal variables with larger amplitudes. Pawlak et al. (2014) distinguished three PL sequences, designated E1–E3, of which sequence E2 consists of systems with two red giant stars, sequence E3 is composed of giant–dwarf binaries, and sequence E1 is a mixture of the previous two types of binary systems.

https://doi.org/10.1017/S1743921323002557 Published online by Cambridge University Press

Lavender dots in Figure 6 represent ellipsoidal variables that do not satisfy the PL relation for close binary systems containing red giants (sequence E). These are so-called heartbeat stars, which are ellipsoidal variables with eccentric orbits (Soszyński et al. 2004). The term 'heartbeat' stars was coined by Thompson et al. (2012), since the light curves of these variables resemble electrocardiogram signatures. The orbital periods of heartbeat stars are naturally longer than those of similar binary systems in circular orbits. The greater the eccentricity of the system's orbit, the larger the displacement of the star relative to sequence E (Wrona et al. 2022a). Recently, Wrona et al. (2022b) published a catalog of nearly 1000 heartbeat stars found in the OGLE photometric database. Tidally excited oscillations have been detected in some of these stars.

9. Long Secondary Periods in Red Giant Stars

The final type of variable stars discussed in this article is the most mysterious one. Long secondary periods (LSPs) occur in at least 30% of LPVs (red giant and supergiant stars) and form a PL relationship designated by Wood as sequence D (blue points in Figure 6). LSPs are roughly ten times longer than the pulsation periods of the same stars and, contrary to their name, are often associated with larger amplitudes of light variations than stellar pulsation (for an example light curve, see the bottom right panel of Figure 6). The LSP phenomenon has been observed for many decades (e.g., O'Connell 1933; Payne-Gaposchkin 1954; Houk 1963), but until recently its origin was completely unknown. Possible explanations of the LSP phenomenon that have been considered in the literature include radial or non-radial stellar pulsations, binarity, episodic dust ejections, turnover of giant convective cells, and magnetic activity.

The first clue that LSPs are related to binarity was provided by the PL diagram, where sequence D partially overlaps and is a continuation of sequence E, populated by close binary systems (Soszyński et al. 2004). However, radial velocity measurements (e.g., Hinkle et al. 2002; Wood et al. 2004) suggested that the hypothetical companion of an LSP red giant should be a brown dwarf or very-low-mass stellar object, which was inconsistent with the so-called 'brown dwarf desert' – an observed deficit of brown dwarf companions to main-sequence stars (Grether & Lineweaver 2006; Nicholls et al. 2009).

A strong argument in favor of the binary origin of the LSP phenomenon was provided by Soszyński et al. (2021), who detected secondary eclipses in their mid-infrared light curves (Figure 7). It is interesting that the secondary eclipses are not visible in the optical range. According to the binary model, an extended cloud of dust is formed around the red giant's low-mass companion, regularly obscuring the main component of the system causing the primary eclipses that are visible in the optical and infrared wavelengths. When the cloud surrounding the brown dwarf passes behind the red giant, the secondary eclipse is visible only in the infrared light curve. To reconcile the brown dwarf desert with a large fraction (at least 30%) of substellar objects accompanying red giants, it should be assumed that brown dwarfs are former planets that have accreted material lost by their parent stars via stellar winds. If this hypothesis were true, it would mean that LSP variables can be used as tracers of planetary systems in the Milky Way and other galaxies. Using the PL relation of LSP stars, it would even be possible to study the three-dimensional distribution of former planetary systems in various stellar environments.

10. Summary

Studies of the PL, PLC, and PW relationships in nearby galaxies are of crucial importance for the calibration of the distance ladder and, therefore, for the confirmation of the Hubble tension. The diverse chemical compositions, different spatial structures, and star

https://doi.org/10.1017/S1743921323002557 Published online by Cambridge University Press

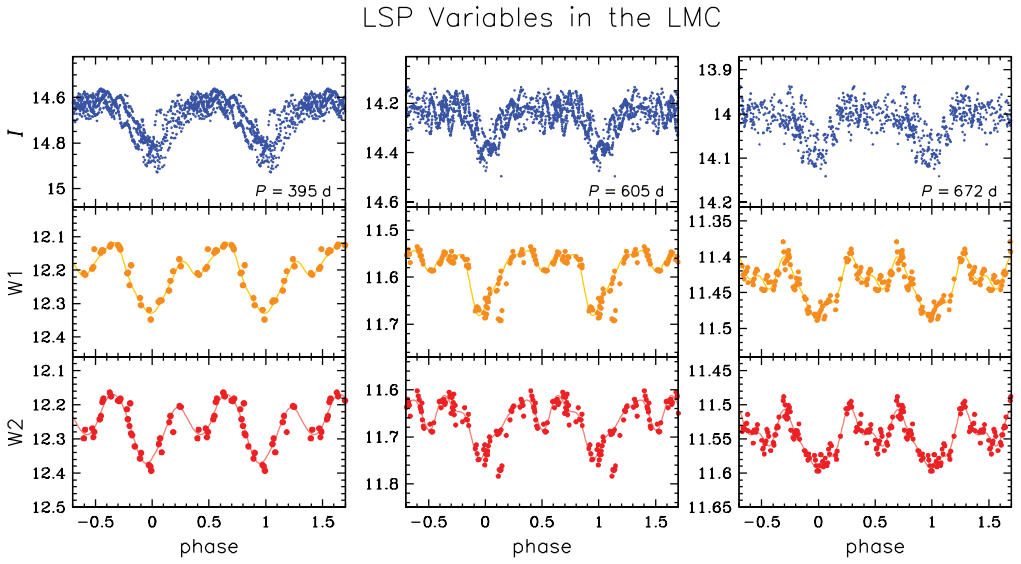

Figure 7. Folded light curves of three LSP variables in the LMC. The top panels show OGLE *I*-band (0.8 μm); middle panels, *WISE W*1 (3.4 μm); and bottom panels, *WISE W*2 (4.6 μm) photometry. The primary minima visible in all wavebands (at phases 0 and 1) are caused by eclipses of the red giant by an orbiting cloud of dust. The secondary minima, visible only in the mid-infrared light curves (at phase 0.5), occur when the cloud is hidden behind the red giant.

formation histories observed in Local Group galaxies provide us with valuable opportunities to explore various aspects, including the influence of metallicity and the linearity of the PL relations on Hubble constant measurements. This will be particularly significant in the face of current and upcoming large telescopes, like the *James Webb Space Telescope* and the Vera C. Rubin Observatory.

However, the PL relations in our closest galactic neighborhood serve a broader purpose, beyond distance measurement. In this work, we have presented examples of applications of the PL, PLC, and PW diagrams to classify variable stars, to discover new types of variables, to elucidate the origins of their light changes, to identify pulsation modes conclusively, to search for binary systems hosting pulsators, and to investigate the three-dimensional geometry of galaxies.

Acknowledgements. This work has been funded by the National Science Centre, Poland, through grant 2022/45/B/ST9/00243. For the purpose of Open Access, the author has applied a CC-BY public copyright licence to any Author Accepted Manuscript (AAM) version arising from this submission.

References

Alcock, C., et al. 1995, AJ, 109, 1653
Anderson, R. I., Koblischke, N. W., & Eyer, L. 2023, arXiv:2303.04790
Arp, H. 1960, AJ, 65, 404
Baade, W. 1954, Trans. IAU, 8, 397
Baade, W. 1956, PASP, 68, 5
Barac, N., Bedding, T. R., Murphy, S. J., & Hey D. R 2022, MNRAS, 516, 2080
Beaulieu, J. P., et al. 1995, A&A, 303, 137
Bhardwaj, A., Kanbur, S. M., Macri, L. M., Singh H. P., Ngeow C.-C., & Ishida E. E. O 2016, MNRAS, 457, 1644
Bhardwaj, A., Macri, L. M., Rejkuba, M., Kanbur S. M., Ngeow C.-C., & Singh H. P. 2017, AJ, 153, 154

https://doi.org/10.1017/S1743921323002557 Published online by Cambridge University Press

Bhardwaj, A., et al. 2019, ApJ, 884, 20
Bhardwaj, A., et al. 2023, ApJL, 944, L51
Bono, G., Caputo, F., Santolamazza, P., Cassisi S., & Piersimoni A. 1997, AJ, 113, 2209
Bono, G., et al. 2019, ApJ, 870, 115
Borissova, J., Rejkuba, M., Minniti, D., Catelan M., & Ivanov V. D. 2009, A&A, 502, 505
Braga, V. F., et al. 2016, AJ, 152, 170
Breuval, L., et al. 2021, ApJ, 913, 38
Breuval, L., Riess, A. G., Kervella, P., Anderson R. I., & Romaniello M. 2022, ApJ, 939, 89
Breuval, L., et al. 2023, ApJ, 951, 118
Chen, X., de Grijs, R., & Deng, L. 2016, ApJ, 832, 138
Chen, X., Deng, L., de Grijs, R., Wang S., & Feng Y. 2018, ApJ, 859, 140
Chown, A. H., Scowcroft, V., & Wuyts, S. 2021, MNRAS, 500, 817
Cioni, M.-R. L., et al. 2011, A&A, 527, A116
Clementini, G., et al. 2019, A&A, 622, A60
Clementini, G., et al. 2023, A&A, 674, A18
Cohen, R. E. & Sarajedini, A. 2012, MNRAS, 419, 342
Connolly, L. P. 1980, PASP, 92, 165
Cusano, F., et al. 2021, MNRAS, 504, 1
Cutri, R. M., et al. 2003, The 2MASS All Sky Point Source Catalog, IPAC, Pasadena
Deb, S. & Singh, H. P. 2014, MNRAS, 438, 2440
Deb, S., Ngeow, C.-C., Kanbur, S. M., Singh H. P., Wysocki D., & Kumar S. 2018, MNRAS, 478, 2526
Ferguson, P. S. & Strigari, L. E. 2020, MNRAS, 495, 4124
García-Varela, A., Sabogal, B. E., & Ramírez-Tannus, M. C. 2013, MNRAS, 431, 2278
Garg, A., et al. 2010, AJ, 140, 328
Gieren, W., et al. 2018, A&A, 620, A99
Glass, I. S. & Evans, T. L. 1981, Nature, 291, 303
Graczyk, D., et al. 2020, ApJ, 904, 13
Grether, D. & Lineweaver, C. H. 2006, ApJ, 640, 1051
Groenewegen, M. A. T. & Jurkovic, M. I. 2017, A&A, 603, A70
Groenewegen, M. A. T. 2018, A&A, 619, A8
Hertzsprung, E. 1913, Astron. Nachr., 196, 201
Hinkle, K. H., Lebzelter, T., Joyce, R. R., & Fekel F. C. 2002, AJ, 123, 1002
Houk, N. 1963, AJ, 68, 253
Huang, C. D., et al. 2020, ApJ, 889, 5
Hubble, E. P. 1925, Pop. Astron., 33, 252
Hubble, E. 1929, PNAS, 15, 168
Inno, L., et al. 2016, ApJ, 832, 176
Ivanov, G. R. & Nikolov, N. S. 1976, Astrophys. Lett., 17, 115
Iwanek, P., Soszyński, I., & Kozłowski, S. 2021, ApJ, 919, 99
Iwanek, P., et al. 2022, ApJS, 260, 46
Iwanek, P., et al. 2023, ApJS, 264, 20
Jacyszyn-Dobrzeniecka, A. M., et al. 2016, Acta Astron., 66, 149
Jacyszyn-Dobrzeniecka, A. M., et al. 2017, Acta Astron., 67, 1
Jayasinghe, T., et al. 2020, MNRAS, 493, 4186
Kanbur, S. M., Ngeow, C., Nanthakumar, A., & Stevens R. 2007, PASP, 119, 512
Kato, D., et al. 2007, PASJ, 59, 615
Leavitt, H. S. 1908, Ann. Harvard Coll. Obs., 60, 87
Leavitt, H. S. & Pickering, E. C. 1912, Harvard Coll. Obs. Circ., 173
Li, S., Riess, A. G., Busch, M. P., Casertano S., Macri L. M., & Yuan W. 2021, ApJ, 920, 84
Macri, L. M., Ngeow, C.-C., Kanbur, S. M., Mahzooni S., & Smitka M. T. 2015, AJ, 149, 117
Madore, B. F. 1982, ApJ, 253, 575
Manick, R., Van Winckel, H., Kamath, D., Sekaran S., & Kolenberg K. 2018, A&A, 618, A21
Marconi, M., Fiorentino, G., & Caputo, F. 2004, A&A, 417, 1101

https://doi.org/10.1017/S1743921323002557 Published online by Cambridge University Press

Martínez-Vázquez, C. E., et al. 2016, MNRAS, 461, L41
Martínez-Vázquez, C. E., Salinas, R., Vivas, A. K., & Catelan M. 2022, ApJL, 940, L25
Muraveva, T., et al. 2015, ApJ, 807, 127
Muraveva, T., et al. 2018, MNRAS, 473, 3131
Nagarajan, P., Weisz, D. R., & El-Badry, K. 2022, ApJ, 932, 19
Neeley, J. R., et al. 2019, MNRAS, 490, 4254
Ngeow, C., Kanbur, S. M., & Nanthakumar, A. 2008, A&A, 477, 621
Ngeow, C.-C., Kanbur, S. M., Neilson, H. R., Nanthakumar A., & Buonaccorsi J. 2009, ApJ, 693, 691
Ngeow, C.-C., et al. 2021, AJ, 162, 63
Ngeow, C.-C., Bhardwaj, A., Graham, M. J., Healy B. F., Laher R. R., Riddle R., & Wold A. 2023, AJ, 165, 190
Nicholls, C. P., Wood, P. R., Cioni, M.-R. L., & Soszyński I. 2009, MNRAS, 399, 2063
O'Connell, D. J. K. 1933, Harvard Coll. Obs. Bull., 893, 19
Ou, J.-Y., Ngeow, C.-C., Bhardwaj, A., Graham M. J., Laher R. R., Masci F. J., & Riddle R. 2023, AJ, 165, 137
Pawlak, M., et al. 2014, Acta Astron., 64, 293
Pawlak, M. 2016, MNRAS, 457, 4323
Payne-Gaposchkin, C. 1954, Ann. Harvard Coll. Obs., 113, 189
Pietrzyński, G., et al. 2010, Nature, 468, 542
Pietrzyński, G., et al. 2019, Nature, 567, 200
Pilecki, B., Pietrzyński, G., Anderson, R. I., Gieren, W., Taormina, M., Narloch, W., Evans, N. R., & Storm, J. 2021, ApJ, 910, 118
Pilecki, B., et al. 2022, ApJL, 940, L48
Poleski, R., et al. 2010, Acta Astron., 60, 1
Ren, Y., Jiang, B.-W., Yang, M., & Gao J. 2019, ApJS, 241, 35
Riess, A. G., Casertano, S., Yuan, W., Macri L. M., & Scolnic D. 2019, ApJ, 876, 85
Ripepi, V., et al. 2017, MNRAS, 472, 888
Ripepi, V., Molinaro, R., Musella, I., Marconi M., Leccia S., & Eyer L. 2019, A&A, 625, A14
Ripepi, V., et al. 2020, A&A, 642, A230
Ripepi, V., et al. 2022, MNRAS, 512, 563
Rucinski, S. M. 1994, PASP, 106, 462
Rucinski, S. M. & Duerbeck, H. W. 1997, PASP, 109, 1340
Rucinski, S. M. 2004, New Astron. Rev., 48, 703
Sandage, A. & Tammann, G. A. 1968, ApJ, 151, 531
Shapley, H. 1918, ApJ, 48, 89
Skowron, D. M., et al. 2021, ApJS, 252, 23
Smolec, R., Moskalik, P., Plachy, E., Soszyński I., & Udalski A. 2018, MNRAS, 481, 3724
Soszyński, I., et al. 2004, Acta Astron., 54, 347
Soszyński, I., et al. 2007, Acta Astron., 57, 201
Soszyński, I., et al. 2008a, Acta Astron., 58, 163
Soszyński, I., et al. 2008b, Acta Astron., 58, 293
Soszyński, I., et al. 2009, Acta Astron., 59, 239
Soszyński, I., et al. 2015, Acta Astron., 65, 233
Soszyński, I., et al. 2016a, Acta Astron., 66, 131
Soszyński, I., et al. 2016b, MNRAS, 463, 1332
Soszyński, I., et al. 2017, Acta Astron., 67, 103
Soszyński, I., et al. 2018, Acta Astron., 68, 89
Soszyński, I., Smolec, R., Udalski, A., & Pietrukowicz P. 2019a, ApJ, 873, 43
Soszyński, I., et al. 2019b, Acta Astron., 69, 87
Soszyński, I., et al. 2020, Acta Astron., 70, 101
Soszyński, I., et al. 2021, ApJL, 911, L22
Soszyński, I., et al. 2022, Acta Astron., 72, 245
Soszyński, I., et al. 2023, Acta Astron., 73, 105

Szabados, L., Kiss, L. L., & Derekas, A. 2007, A&A, 461, 613
Thompson, S. E., et al. 2012, ApJ, 753, 86
Trabucchi, M., Mowlavi, N., & Lebzelter, T. 2021, A&A, 656, A66.
Udalski, A., Soszyński, I., Szymański, M., Kubiak M., Pietrzyński G., Woźniak P., & Żebruń K. 1999, Acta Astron., 49, 223
Udalski, A., Szymański, M. K., & Szymański, G. 2015a, Acta Astron., 65, 1
Udalski, A., et al. 2015b, Acta Astron., 65, 341
Udalski, A., et al. 2018, Acta Astron., 68, 315
Werner, M. W., et al. 2004, ApJS, 154, 1
Wielgórski, P., et al. 2017, ApJ, 842, 116
Wielgórski, P., et al. 2022, ApJ, 927, 89
Wood, P. R. & Sebo, K. M. 1996, MNRAS, 282, 958
Wood, P. R., et al. 1999, Proc. IAU Symp., 191, 151
Wood, P. R., Olivier, E. A., & Kawaler, S. D. 2004, ApJ, 604, 800
Wright, E. L., et al. 2010, AJ, 140, 1868
Wrona, M., Kołaczek-Szymański, P. A., Ratajczak, M., & Kozowski, S. 2022a, ApJ, 928, 135
Wrona, M., et al. 2022b, ApJS, 259, 16
Yuan, W., Macri, L. M., Javadi, A., Lin Z., & Huang J. Z. 2018, AJ, 156, 112
Ziaali, E., Bedding, T. R., Murphy, S. J., Van Reeth T., & Hey D. R. 2019, MNRAS, 486, 4348
Zinn, R. & Searle, L. 1976, ApJ, 209, 734

Discussion

Question (Martínez-Vázquez): I have a question regarding the PLR in δ Scuti stars. Did you see the same two sequences in the Galactic bulge δ Scuti stars as you showed for the LMC?

Answer: I have not studied it thoroughly. At first glance, there is no double PL relation in the Galactic bulge, which is understandable owing to the large depth of the bulge along the line of sight, which significantly broadens the PL relations.

Question (Braga): You showed us that the I-band PLR of δ Scuti stars does not show any break in the slope, as did the V-band PL relation of Martínez-Vázquez. Since OGLE also has V-band data, can you tell us what the PL(V) looks like in OGLE?

Answer: In the V band, the PL diagram for δ Scuti stars in the LMC looks essentially the same as in the I band (there are two linear relationships), only the scatter is larger.

Question (Braga): You showed ultra-faint RV Tau light curves, and they were folded at twice the period, as usually done for RV Tau stars, with alternating deep/shallow minima. However, those two light curves did not look like they showed alternating minima. Did you use twice the period for all RV Tau stars for your PLRs?

Answer: Good question. During my talk, I presented pre-whitened light curves of these two stars (corrected for period changes and long-term brightness modulations). To see the original light curve, please check Figure 6 in the paper of Soszyński et al. (2018). Alternating deeper and shallower minima are not always obvious in RV Tauri (or related) stars. In the case of OGLE-LMC-T2CEP-237, the alternations are visible, while for OGLE-LMC-T2CEP-207 we can see long-term changes of the mean magnitudes, as is observed in RV Tauri-type b (RVb) stars.

https://doi.org/10.1017/S1743921323002557 Published online by Cambridge University Press